Mol Gen Genomics (2005) 272: 639–650
DOI 10.1007/s00438-004-1085-6

ORIGINAL PAPER

B. Leuthner · C. Aichinger · E. Oehmen
E. Koopmann · O. Müller · P. Müller · R. Kahmann
M. Bölker · P. H. Schreier

A H_2O_2-producing glyoxal oxidase is required for filamentous growth and pathogenicity in *Ustilago maydis*

Received: 2 June 2004 / Accepted: 20 October 2004 / Published online: 1 December 2004

Abstract In the phytopathogenic fungus *Ustilago maydis* the mating-type loci control the transition from yeast-like to filamentous growth required for pathogenic development. In a large REMI (restriction enzyme mediated integration) screen, non-pathogenic mutants were isolated in a haploid strain that had been engineered to be pathogenic. In one of these mutants, which showed a specific morphological phenotype, the tagged gene, *glo1*, was found to encode a product that is highly homologous to a glyoxal oxidase gene from the wood-rot fungus *Phanerochaete chrysosporium*. Glyoxal oxidase homologues are found in human, plant pathogenic fungi and in plants, but not in other mammals or yeasts. To confirm the function of the *glo1* gene, null mutations were generated in compatible haploid *U. maydis* strains. In crosses null mutants were unable to generate filamentous dikaryons, and were completely non-pathogenic. Using a Glo1-overproducing strain we demonstrated that Glo1 is membrane bound, oxidizes a series of small aldehydes ($<$C4) and produces H_2O_2. The enzyme needs to be activated, presumably by auto-oxidation, to show full activity. A potential role for Glo1 during filamentous growth and pathogenic development of *U. maydis* is proposed.

Keywords Deletion mutant · Gene knock-out · Overproduction · Protein

Electronic Supplementary Material Supplementary material is available in the online version of this article at http://dx.doi.org/10.1007/s00438-004-1085-6

Communicated by P. J. Punt

The first two authors contributed equally to this work
We dedicate this work to the memory of Jeff Schell, a charismatic and outstanding person who loved science and respected people

B. Leuthner · C. Aichinger · E. Oehmen · E. Koopmann
P. H. Schreier (✉)
Bayer CropScience AG, Alfred-Nobel-Strasse 50,
40789 Monheim, Germany
E-mail: peter.schreier@bayercropscience.com
Tel.: +49-2173-384514
Fax: +49-2173-383520

O. Müller
Department of Plant Breeding and Yield Physiology,
Max Planck Institute for Plant Breeding Research,
Carl-von-Linné Weg, 50829 Köln, Germany

P. Müller · R. Kahmann
Department of Organismic Interactions,
Max Planck Institute for Terrestrial Microbiology,
Karl-von-Frisch-Strasse, 35043 Marburg, Germany

M. Bölker
Department of Biology, Philipps-Universität Marburg,
Karl-von-Frisch-Strasse 8, 35032 Marburg, Germany

Present address: B. Leuthner
Direvo Biotech AG, Nattermannallee 1,
50829 Köln, Germany

Present address: C. Aichinger
Roche Diagnostics GmbH, Nonnenwald 2,
82372 Penzberg, Germany

Introduction

Corn smut disease is caused by the phytopathogenic basidiomycete *Ustilago maydis*. For pathogenic development to occur, haploid cells need to fuse and to grow as filamentous dikaryons. Cell fusion, the dimorphic switch to filamentous growth, and pathogenic development are governed by the two unlinked mating-type loci *a* and *b*. The biallelic *a* locus encodes a pheromone receptor system (Bölker et al. 1992; Spellig et al. 1994). The pheromone signal, which is a prerequisite for cell fusion and generation of the dikaryon, is transmitted via a MAP kinase cascade. MAP kinase null mutants are unable to grow filamentously and remain in a yeast-like form (Müller et al. 1999). Maintenance of the dikaryon, filamentous growth and subsequent pathogenic development are controlled by the *b* locus, which encodes two different homeodomain proteins, bE and bW, which dimerize only when they originate from different alleles. The bE/bW heterodimer acts as a transcription factor

for a large number of genes (Brachmann et al. 2001; Romeis et al. 2000).

Cell fusion and sexual development are initiated under specific environmental conditions, and involve tight regulation of the intracellular cAMP level. Thus, mutants defective in cAMP signalling display abnormal cell morphology, and are affected in dikaryon formation and pathogenicity (Gold et al. 1994; Krüger et al. 1998). The importance of the dimorphic switch for pathogenicity was demonstrated by the isolation of mutants that affect a motor protein and the vesicle transport system, which showed both impaired filamentous growth and reduced virulence of the dikaryon (Lehmler et al. 1997; Wedlich-Söldner et al. 2002). In other systems also, abnormal morphology is often linked to reduced virulence or complete loss of pathogenicity (Giasson and Kronstad 1995; Lau and Hamer 1998).

Tagging mutagenesis by restriction enzyme mediated integration (REMI) (Schiestl and Petes 1991) allows the identification of genes involved in traits, such as virulence, which are not amenable to gene isolation via complementation. Genes tagged by the inserted DNA can be rapidly isolated by plasmid rescue. To confirm that the insertion is coupled to the observed phenotype the isolated plasmid is used to generate the same mutation in the parental strain by homologous recombination, or a knock-out mutant for the tagged gene can be generated in the parental strain by gene replacement.

The genetically modified haploid *U. maydis* strain CL13 expresses an active bE/bW heterodimer and hence does not need to fuse in order to infect plants and induce tumor formation. Thus, CL13 is suitable for the isolation of pathogenicity mutants, and has been used in a REMI screen for such mutants (Bölker et al. 1995a). Some of the non-pathogenic mutants identified in this screen showed additional morphological phenotypes.

In this study we describe the characterization of the *U. maydis* gene *glo1* (Accession No. AJ550625), which encodes a glyoxal oxidase. Members of this class of enzymes have previously been identified only in the white rot fungus *Phanerochaete chrysosporium* as components of the lignin degradation pathway (Kersten and Kirk 1987; Kersten et al. 1995). *U. maydis* has two additional genes homologous to *glo1*: *glo2* (AJ550626) and *glo3* (AJ550627). Deletion of either of these genes did not lead to any obvious phenotypes. We show that the membrane-bound glyoxal oxidase Glo1 is required for pathogenic development and for maintenance of cell morphology and filamentous growth in *U. maydis*.

Materials and methods

Reagents

Chemicals, biochemicals and enzymes were obtained from Roche Diagnostics (Mannheim, Germany), Fluka (Neu-Ulm, Germany), Merck (Darmstadt, Germany), Mobitech (Göttingen, Germany) or Sigma-Aldrich (Deisenhofen, Germany).

Growth conditions for *U. maydis*

Strains were grown at 28°C in PD or YEPS medium (Tsukada et al. 1988). Mating assays were carried out by co-spotting strains onto PD plates containing 1% charcoal. Subsequent incubation was done at 21°C (Holliday 1974).

Pathogenicity assays were carried out as described by Gillissen et al. (1992). Overnight cultures of the *U. maydis* strains were grown to an OD_{600} of 0.8, resuspended to a density of 4×10^7 cells/ml and injected into young corn seedlings (Gaspar Flint). Plants were examined for tumor formation 7–21 days post infection.

For agar diffusion assays, strains were plated on PD medium. Filter disks of Whatman paper (5 mm) or Millipore GS membranes (13 mm) were soaked with 1 µl of H_2O_2 [10% (v/v)], 1 µl of methylglyoxal [MG; 40% (v/v)] or 25 µl of 2.5% (w/v) SDS, and placed on the plates. The sizes of halos corresponding to zones of non-growing cells were measured in eight duplicates for each concentration after 36–48 h of incubation.

DNA and RNA procedures

Standard molecular methods were performed according to Sambrook et al. (1989). A PCR-based strategy was employed to generate *glo1* null mutants (Kämper 2003, 2004). Genomic DNA of the haploid *U. maydis* strain 518 served as the template. A 5′ flanking region of 1151 bp was amplified with the primer pair LB2 (5′-CACGGCCTGAGTGGCCGGTGTGTAAACGA-TCCTTTCTGGAAG-3′) and LB1 (5′-CCTCCAAGT-TTCGAGATATCGACC-3′). A 3′ flanking region of 1249 bp was amplified using the primers RB1 (5′-GTGGGCCATCTAGGCCGTCAACAGCACCA-AATTCACAGCC-3′) and RB2 (5′-ATCGTAGCTCG-AGTGTATGCTTCC-3′). The primers LB2 and RB1 introduce *Sfi* I sites into the amplification products. Amplicons were cleaved with *Sfi* I and ligated to a 1884-bp *Sfi* I fragment containing the hygromycin B cassette from the vector pBS. For transformation, the ligation product of 4300 bp was amplified by PCR using the primers LB1 and RB2. The genes *glo2* and *glo3* were disrupted using a similar procedure. The primer pairs used to knock out *glo2* were glo2_rB2 (5′-TAC-ACGAGGGTCCCAAAGAAGC-3′)/glo2_lB1 (5′-AT-GTTGGCGAAATGGAGGGTCG-3′), and glo2_rB1 (5′-GTGGGCCATCTAGGCCGTCAAGGAAAGAT-GGTCATGGTGG-3′)/glo2_lB2 (5′-CACGGCCTGA-GTGGCCACGCCCGAATTGCCAACGACTTGC-3′), which amplify the right and left borders flanking *glo2*.

For the *glo3* knock-out the primer pairs glo3_rBo2 (5′-TTGCTCATCAGCAGTCTCTG-3′)/glo3_rB1 (5′-GTGGGCCATCTAGGCCGCCTTCGCCCTGTTTG-CTTGATTG-3′) and glo3_lB2 (5′-CACGGCCTGAG-TGGCCGACGATGCAGCCATTACGACGAGG-3′)/ glo3_lBo1 (5′-TGTGCTTGAGGATCGTCAG-3′) were used.

Transformation of *U. maydis* was carried out according to Schulz et al. (1990). Isolation of genomic DNA from *U. maydis* is described by Hoffmann and Winston (1987). Transformants were checked by Southern hybridization analysis.

Plasmid rescue was carried out as described by Bölker et al. (1995a). Genomic DNA of the *U. maydis* CL13 (*a1bE1*/ *bW2*) strain 5662 was cleaved with *Mlu* I, religated and used to transform *E. coli* cells via electroporation.

For overproduction of Glo1 a 3400-bp fragment encompassing the *glo1* gene was amplified with the primers 5'glo1 (5′-CCCGGGATGACGAGGCACCT-CTCCTCATC-3′), which includes the start codon of *glo1* (underlined), and primer 3'glo1Not (5′-GCGG-CCGCGAATTGGTCAGACGAATCCG-3′) which anneals 0.6 kb downstream of the *glo1* ORF. The amplicon was cloned into pCR-Topo2.1. The *glo1* fragment was re-isolated by restriction with *Sma* I and *Not* I, and transferred into the respective sites of pCA123 (for sequence, see Electronic Supplementary Material). The resulting plasmid, pCA929, was linearized by digestion *Ssp* I, and transformed into *U. maydis* 518Δglo1. Strains containing the construct were selected for carboxin (Cbx) resistance (Keon et al. 1991).

For localization studies of Glo1 the coding region of *glo1* was amplified with the primers Glo1-GFPfwd (5′-ATGACGAGGCACCTCTCCTCATC-3′) and Glo1-GFPrev (5′-GCGTCGACTAGAGTAGCTTCCTT-GG-3′). The amplicon was fused to the 5′ end of the gene encoding eGFP by insertion into the *Sma* I site of pCA123. The resulting construct, glo1-GFP, was then transformed into *U. maydis* strain 521.

To investigate the role of Glo1 in cAMP signalling, an *U. maydis* Um521Δglo1Δadr1 strain was generated: To delete the *adr1* gene, its 5′ and 3′ regions were amplified with the primer pairs adr1-894 (5′-GCCGC-TGCTGTTACTCATG-3′)/adr1-5'SfiI (5′-CTGGGCC-ATCTAGGCCATCTACGGAAACGGTAGAGCTC-G-3′), and adr1 + 2262 (5′-GACGATCGATCGGATG-C-3′) and adr1-3'SfiI (5′-TGAGGCCTGAGTGGCCG-GCTGGCTCAACACGCGCATACC-3′). After cleavage with *Sfi* I these fragments were ligated with an *Sfi* I-cleaved 2.4-kb phleomycin resistance cassette isolated from pBS-phleo (Brachmann et al. 2004). The ligation product was subsequently cloned into pCR-TOPO2.1, resulting in pCRΔadr1phleo. To generate the Um521Δ–glo1Δadr1 double mutant, Um521Δglo1 was transformed with the PCR product amplified with the primers adr1-894 and adr1 + 2202, using pCRΔadr1phleo as template. Two independent Um521Δglo1Δadr1 strains were verified by Southern analysis.

cAMP treatment

The strains CA95 and FB2 (Table 1) were grown in CM + 1% glucose supplemented with 15 mM cAMP for 16 h to an OD_{600} of 0.6.

Glo1 activity assay

Glyoxal oxidase activity was determined in culture supernatants, whole cells, cell extracts and membrane fractions. Cells were grown in minimal medium to an OD_{600} of 0.7, harvested and resuspended to an OD_{600} of 50 in 50 mM TRIS-HCl (pH 8). Cell extracts were prepared by suspending protoplasts of the *U. maydis* strains in distilled water. All subsequent steps were carried out at 4°C. Cell debris was removed by centrifugation at 8000 rpm. The membrane fraction was collected by centrifugation at 13,000 rpm for 30 min. The membrane pellet was resuspended in 500 µl of

Table 1 Strains used in this study

Strain	Genotype	Reference or source
Um518	*a2 b2*	R. Holliday
Um521	*a1 b1*	R. Holliday
Um521Glo1eGFP	*a1 b1 Potef::glo1-gfp Cbx* ^{R}	This study
Um521eGFP	*a1 b1 Potef::gfp Cbx* ^{R}	This study
Um518Δglo1	*a2 b2* Δglo1::Hyg	This study
Um521Δglo1	*a1 b1* Δglo1::Hyg	This study
Um518Δglo2	*a2 b2* Δglo2::Hyg	This study
Um521Δglo2	*a1 b1* Δglo2::Hyg	This study
Um518Δglo3	*a2 b2* Δglo3::Hyg	This study
Um521Δglo3	*a1 b1* Δglo3::Hyg	This study
SG200	*a1:mfa2 bE1/bW2*	Bölker et al. (1995b)
SG200Δglo1	*a1:mfa2 bE1/bW2* Δglo1::Hyg	This study
CA95	*a2 b2* Δglo1 Potef::glo1 Cbx ^{R}	This study (derived from Um518)
CL13	*a1bE1/bW2*	Bölker et al. (1995a)
Um521Δglo1Δadr1	*a1 b1* Δglo1 Δadr1::Hyg	This study
FB2	*a2 b2*	Banuett and Herskowitz (1989)
FB2Δadr1	*a2 b2* Δadr1::Hyg	Dürrenberger et al. (1998)

50 mM TRIS-HCl (pH 8) or 180 µl of the same buffer containing 1.5% (v/v) Tween-20 (substrate spectrum experiment). The efficiency of cell fractionation was tested by assaying for glyceraldehyde-3-phosphate (GAPDH) activity (determination of NADH production in the presence of AsO_4^{3-}, NAD and GAP) using identical volumes of membrane and cytosolic fractions. For the Glo activity test 1-µl aliquots of membrane suspension were used, for the substrate spectrum 4-µl samples. Glyoxal oxidase activity was determined using a coupled assay with horseradish peroxidase (HRP) and phenol red. The reaction mixture (50 µl) contained 10 µl of sample, 12 mM dimethylsuccinate buffer (pH 5), 10 mM MG, 19 U of HRP and 0.001% (w/v) phenol red (Kersten and Kirk 1987). Reaction mixtures were incubated at 28°C. Reactions were stopped after 16 h by adding 20 µl of 1 M NaOH. The A_{550} values were then determined spectrometrically.

For determination of substrate specificity substrates (short-chain alcohols and aldehydes, sugars, β-hydroxyaldehydes and -ketones, α-, β-dicarbonyl compounds) were added at final concentrations of 2 mM and 10 mM.

Alternatively, enzymatic activity was determined by coupling the production of H_2O_2 via HRP to the oxidation of Amplex Red (Molecular Probes). The coupling reaction was carried out according to the manufacturer's instructions, with slight modifications. Reaction volume was 50 µl. CA95 and Um518 cells were harvested, washed with water and transferred to microtiter plates to give a final OD_{600} of 1. The reaction was started by the addition of MG (MG; final concentration 10 mM). After incubation at 30°C for 9 h, the reaction products were detected fluorimetrically, using an excitation wavelength of 550 nm and emission at 595 nm, in a Tecan plus fluorescence reader. Measurements were repeated eight times and the experiments were done in duplicate.

Imaging

Microscopic examination of *U. maydis* strains was carried out using a Zeiss Axioskop with differential interference contrast (DIC) optics. Plates were photographed with a Casio CCD camera. Pictures were processed using Adobe Photoshop 5.0 and Microsoft Power Point. For the analysis of eGFP fusion proteins, the Um521-glo1-GFP strain was grown in CM + 1% glucose to an OD_{600} of 0.6, and cells were embedded in 1% low-melting agarose (Sigma A-4018) for microscopic examination. Pictures were taken using a CCD camera (C4742-95; Hamamatsu). GFP and Calcofluor were detected by fluorescence microscopy using specific filter sets (BP 470/20, FT 493, BP 505–530; Zeiss) and (BP 395–440, FT 460, LP > 470) respectively. Image processing and measurements were done with Axiovision 3.1 (Zeiss) and Canvas 7.0 (Deneba).

Results

REMI integration identifies an ORF whose predicted product shows significant homology to glyoxal oxidases

Among the REMI mutants affected in pathogenicity recovered in the screen performed by Bölker et al. (1995a), we chose for further analysis one that showed an additional morphological phenotype. This mutant formed fluffy colonies. The cells exhibited a pleiotropic morphology defect—appearing distorted and showing a higher degree of vacuolation than wild-type cells. Plasmid rescue led to the isolation of a 5490-bp genomic fragment, and the insertion was mapped 770 bp downstream of the start codon of a putative ORF. The 862-amino acid sequence deduced from this ORF showed significant homology to that of the glyoxal oxidase-encoded by the *glx* genes from *Phanerochaete chrysosporium*. We therefore assigned the symbol *glo1* (glyoxal oxidase1) to the *U. maydis* gene.

A search of the *U. maydis* genome sequence identified two additional glyoxal oxidase homologues, *glo2* (1878 bp) and *glo3* (1959 bp) (see Fig. 1A for a schematic representation of their organization). Their products show 42% and 38% sequence identity, respectively, to Glo1. In silico analysis predicted that Glo2 is most likely to be a secreted protein, while Glo1 and Glo3 contain a putative transmembrane domain and a GPI anchor, respectively. Interestingly, for Glo3 the iPSORT algorithm (Nakai and Horton 1999) predicted a cytoplasmic localization of the catalytic domain, while the catalytic portion of Glo1 is most probably extracellular. All three *U. maydis* proteins share not only overall similarity with Glx2 (29% identity to Glo1, 30% to Glo2 and 28% to Glo3) but also a conserved Cu^{2+} binding domain which defines the redox centre of Glx1/Glx2 (Fig. 1A). Figure 1B shows a phylogenetic tree based on a ClustalW analysis of all deduced glyoxal oxidase protein sequences from fungi that are currently available in public databases. This tree also includes all galactose oxidase protein sequences, since these proteins also contain the conserved Cu^{2+} binding domain and were demonstrated to have close structural similarities in their active sites (Whittaker et al. 1999). As a point of reference glyoxal oxidase proteins from *Arabidopsis thaliana* are included. The sequences of essential parts of these proteins (residues 1–110, and 320–530) are provided as Electronic Supplementary Material, highlighting the conserved amino acids. In contrast to the recently described copper-radical oxidase gene family in *P. chrysosporium*, where three of the seven genes are clustered within a region of 50 kb (Martinez et al. 2004), the *U. maydis glo* genes are not clustered: *glo1* is found on chromosome V, *glo2* and *glo3* on chromosome II (separated from each other by about 750 kb), while *gao1* (UM02809.1 on supercontig 1.94), a proposed galactose oxidase gene, is located on chromosome VI.

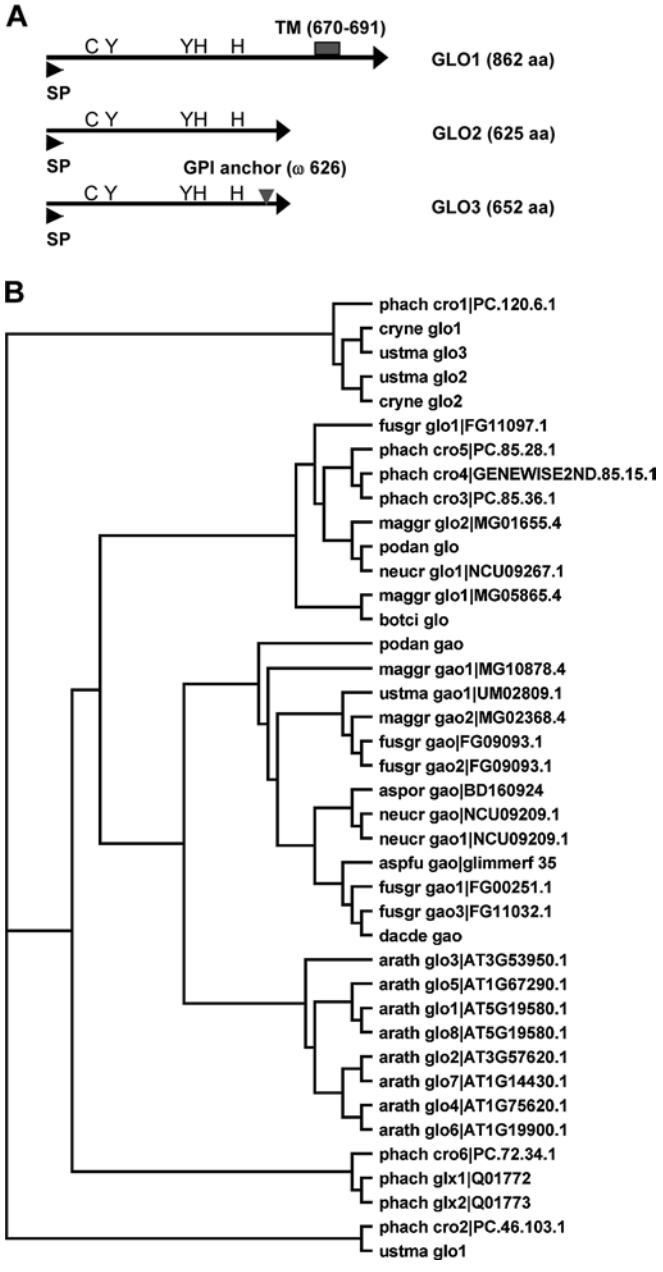

Fig. 1A, B Domain organization of Glo1 (AJ550625), Glo2 (AJ550625) and Glo3 (AJ550627) of *U. maydis* (**A**) and phylogenetic analysis of their homologues in other species (**B**). **A** Conserved residues involved in Cu^{2+} binding, putative signal peptides (SP) and the postulated transmembrane domain (TM) are indicated. **B** A phylogenetic tree based on a ClustalW analysis (CLUSTALX 1.81, Matrix BLOSUM62) is shown. The analysis was performed with sequences either directly taken from protein datasets or obtained by homology searches in the corresponding genomes, followed by conceptual translation. The following sequence sources were used: *Arabidopsis thaliana* (http://www.arabidopsis.org); *Aspergillus oryzae* (GenBank Accession No. BD160924); *Aspergillus fumigatus* (http://www.sanger.ac.uk/Projects/A_fumigatus/), *Cryptococcus neoformans* (http://www-sequence.stanford.edu/group/C.neoformans), *Dactylium dendroides* (Uniprot Accession No. Q01745), *Fusarium graminearum* (http://www.broad.mit.edu/annotation/fungi/fusarium/index.html), *Magnaporthe grisea* (http://www.broad.mit.edu/annotation/fungi/magnaporthe/index.html), *Neurospora crassa* (http://mit.edu/annotation/fungi/neurospora/index.html), *Phanerochaete chrysosporium* (ftp://ftp.jgi-psf.org/pub/JGI_data/WhiteRot/), *Podospora anserina* (http://podospora.igmors.u-psud.fr/download.html), and *Ustilago maydis* (http://www.broad.mit.edu/annotation/fungi/ustilago/index.html). Organisms are abbreviated in accordance with the acronyms used by the SWISSPROT taxonomy (http://www.ebi.ac.uk/newt/index.html)

Glo1 is localized in the plasma membrane

The subcellular localization of Glo1 was determined by the expression of an N-terminal fusion of Glo1 to eGFP. The eGFP-specific signal was detected in patches in the plasma membrane (Fig. 2B II): In young buds the fusion protein was concentrated at the tip, older buds showed a more dispersed signal. Later the protein was localized in septa and bud scars. Additional fluorescence was seen in the vacuole. Both sources of fluorescence correlated with the two signals observed upon immunodetection analysis (Fig. 2B I). The vacuolar staining is most likely to be derived from degradation of the constitutively expressed full-length fusion protein. Recent studies in yeast have demonstrated that, after turnover, GFP-tagged plasma membrane proteins are reimported by endocytosis and targeted to the vacuole for degradation (Petersson et al. 1999; Paiva et al. 2002). Fluorescence microscopy of the otef-eGFP reporter strain, which expresses eGFP alone, showed that eGFP itself is not targeted from the cytosol to the vacuole (Fig. 2B III).

The efficacy of the signal peptide of Glo1 was also confirmed in the heterologous yeast signal sequence trap system (Klein et al. 1996). A fusion protein consisting of the Glo1 signal peptide attached to yeast invertase is effectively secreted in yeast (not shown).

glo1 mutants are mating-deficient and cannot grow filamentously

To study the function of the *glo1* gene, knock-out mutants were generated by gene replacement in the compatible haploid strains Um518 and Um521. Strains deleted for *glo1* formed aggregates of distorted, irregularly branched cells which also showed a cytokinesis defect. Knock-out cells showed similar morphological defects to the REMI mutant. The mutant cells were much shorter than wild-type cells, appeared swollen and showed a high degree of vacuolation (Fig. 2). Despite their severe morphological defects, the growth rates of the mutant strains were not significantly reduced compared to wild type (not shown).

When tested in a plate mating assay, mating-compatible Δglo1 mutants failed to develop the typical white dikaryotic mycelium (Fig. 3A), and the same combination of strains was unable to induce symptoms when injected into corn seedlings (Table 2). However, when *glo1* mutants were co-spotted with compatible wild-type strains, some filaments were observed (Fig. 3A) and

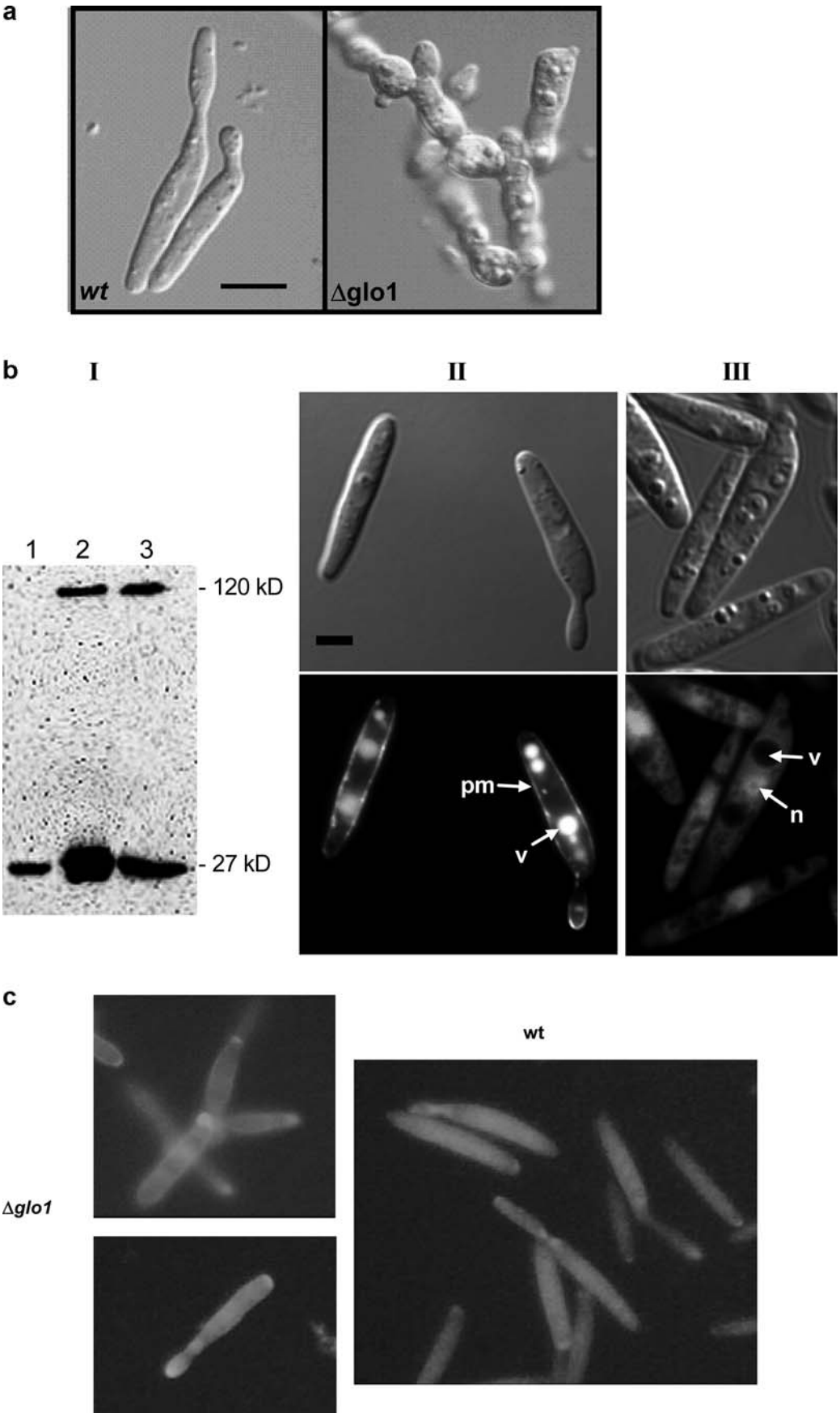
a
wt
Δglo1
b
I
II
III
1
2
3
- 120 kD
- 27 kD
pm
v
v
n
c
wt
Δglo1

◄

Fig. 2A–C Phenotypic analyses of the Um521 *glo1* mutants in comparison to wild type (Um521) cells (wt). **A** Cells were grown in PD medium, washed with water and fixed in 1% (w/v) Kelzan. Scale bar = 3 μm. **B** I. Immunodetection of eGFP in cell extracts of independent *glo1-eGFP* reporter strains. pCA123 without an insertion was integrated as a control (lane 1, strain Um521 *otef-eGFP*); the eGFP migrates at 27 kDa. The Glo1 protein was N-terminally fused to eGFP (lanes 2 and 3; *glo1-eGFP-1,2*) leading to signals at 120 kDa (the size of the fusion protein) and additional signals which may be due to partial degradation. II. Localization of the Glo1-eGFP fusion protein (strain Um521 *glo1-eGFP-1*). The fusion protein is transferred into the secretory pathway and finally localized to the plasma membrane (pm). Degraded protein accumulates in the vacuole (v). Scale bar = 2.5 μm. III. Localization of eGFP (strain Um521 *otef-eGFP*). eGFP is located in the cytosol and accumulates in the nucleus (n) but not in the vacuole. **C** Calcofluor staining of Δ *glo1* and wt cells. Cells were grown in CE medium plus 1% glucose to an OD_{600} value of 0.6. Cells were harvested, resuspended in PBS, and inspected in medium supplemented with 1 μM Calcofluor. Δ *glo1* cells are shown on the *left* and wt cells on the *right*

these mixtures were able to infect corn seedlings (Table 2). This indicates that *glo1* mutants are not completely impaired in cell fusion. In contrast to *glo1* mutant strains, neither *glo2* nor *glo3* null mutants displayed obvious phenotypes (not shown) and were fully pathogenic (Table 2).

glo1 is required for pathogenic development in haploid pathogenic strains

To investigate whether the reduction in filament formation observed in matings of Δglo1 strains is due a post-fusion defect in filamentation, the Δglo1 mutation was introduced into the haploid pathogenic strain SG200 (Table 1) by gene replacement. SG200 is able to grow as a filament on charcoal-containing plates because it carries both the active *b* heterodimer and a self-stimulatory combination of the *a* 1 receptor and *a* 2 pheromone (Bölker et al. 1995b). SG200Δglo1 cells have the same morphology as the haploid Δglo1 Um518 and Um521 derivatives (not shown). On charcoal plates SG200Δglo1 failed to grow filamentously (Fig. 3A, left panel) and was non-pathogenic in corn plants (Table 2). This demonstrates that *glo1* is required for filamentation as well as for pathogenic development.

Overproduction of Glo1 complements the *glo1* phenotype

To overproduce Glo1, we constructed the *glo1-1* allele, allowing the *glo1* gene to be expressed under the control of the constitutive *otef* promoter (Spellig et al. 1996). The *glo1-1* allele was integrated into the *cbx* locus in the *glo1* mutant strain Um518Δglo1. The resulting strain, CA95 (Um518a2b2 Δglo1 glo1-1), was indistinguishable from wild-type cells and formed filaments efficiently when crossed to a compatible wild-type strain (not shown). Tumor formation by CA95 crossed with Um521 was comparable to that seen in crosses of wild-type strains (Table 2).

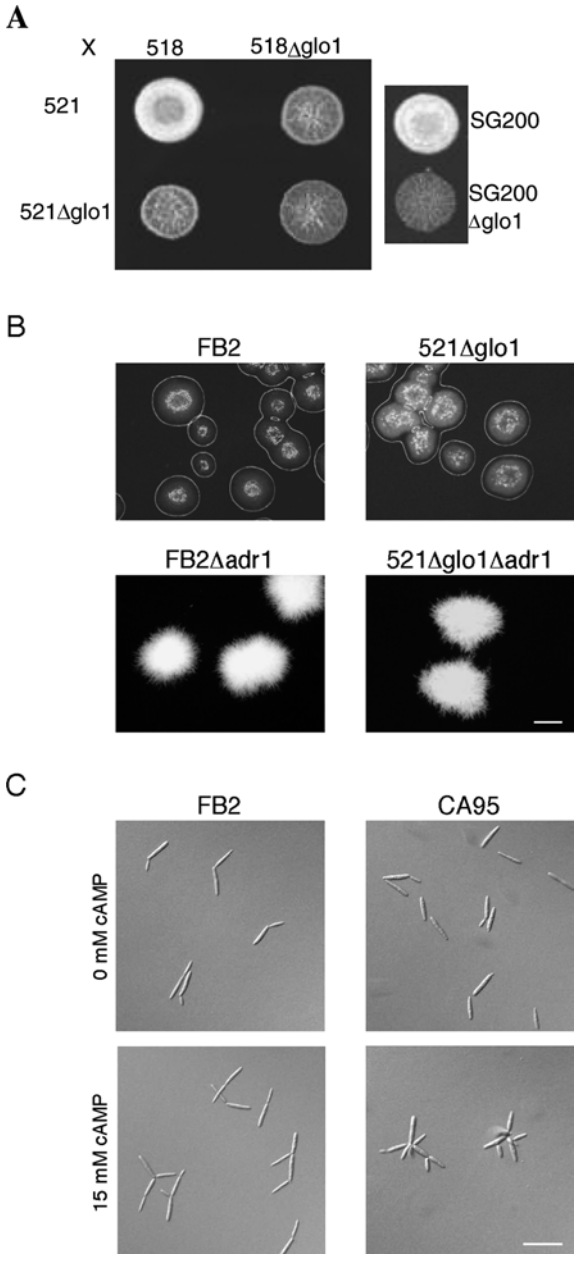

Fig. 3A–C Phenotype of Δ *glo1* strains. Strains were spotted alone or in combination on PD-charcoal plates and incubated for 48 h. **A** The Δ *glo1* allele was introduced into Um521(*a1b1*) or Um518(*a2b2*). Strains were spotted as indicated (*left panel*). The appearance of white mycelium indicates successful mating. The haploid and pathogenic wild type SG200 (*a1:mfa2bE1/ bW2*) strain and the *glo1* mutant strain SG200Δglo1 were spotted separately (*right panel*). Note that all *glo1* mutant strains showed the same colony morphology. **B** Colony morphology of a Δ *adr1*Δ *glo1* strain. The strains indicated *above* the panels were grown on PD-charcoal plates for 48 h. All pictures were taken at the same magnification. Scale bar = 1 mm. **C** Cell morphology of FB2 and CA95 cells upon cAMP treatment. The strains indicated *above* the panels were grown in CM + 1% glucose for 16 h, supplemented with 15 mM cAMP where indicated. All pictures were taken with the same magnification. Scale bar = 20 μm

Table 2 Pathogenicity of *glo1, glo2* and *glo3* mutant strains

Cross	Number of plants inoculated[a]	Number of tumors observed	Percentage
Um518 (*a2b2*) x Um521 (*a1b1*)	117	106	91
Um518 Δglo1 × Um521 Δglo1	330	0	0
Um518 Δglo1 × Um521	26	15	58
Um521 Δglo1 × Um518	41	35	85
SG200 (*a1bE1*/*bW2*)	103	79	77
SG200 Δglo1	239	0	0
CA95 × Um521	44	38	86
Um518 Δglo2 × Um521 Δglo2	182	161	88
Um518 Δglo3 × Um521 Δglo3	82	67	82

[a]For each test at least 20 plants were infected in two independent experiments and with at least two independent transformants

Glo1 appears not to be involved in cAMP signaling

In *U.* maydis cAMP signaling is a critical regulator of cell morphology and filamentous growth (Kahmann et al. 2000). Haploid cells which are impaired in cAMP signaling, e.g. strains deleted for the gene *adr1*, which codes for protein kinase A (PKA) grow filamentously, whereas an activated cAMP cascade leads to a cell separation defect termed multiple budding, which inhibits filamentous growth (Kahmann et al. 2000). To analyze whether the morphological phenotypes of Δ *glo1* cells (severe defects in cell separation and filamentous growth) reflect a function of *glo1* in cAMP signaling, we generated *adr1glo1* double mutants. These mutant strains showed no differences in filamentous growth from *adr1* single knock-out strains (Fig. 3B). On the other hand, cells that overexpress Glo1 react with multiple budding when grown in the presence of exogenous cAMP (Fig. 3C). These results suggest that Glo1 is not a part of the cAMP signaling pathway and influences cell morphology by a different mechanism.

Glo1 produces H_2O_2 using methylglyoxal as substrate

To analyze the enzymatic properties of the Glo1 protein, Um518, the respective *glo1*, *glo2* , *glo3* mutants thereof, and Glo1-overproducing CA95 cells (Table 1) were assayed for their ability to oxidize methylglyoxal (MG) and produce H_2O_2. MG dependent production of hydrogen peroxide can be detected colorimetrically, in a coupled reaction with horseradish peroxidase and phenol red, as a decrease in absorbance at 550/590 nm (Pick and Mizel 1981). In the absence of MG no production of H_2O_2 was observed. Based on the amount of H_2O_2 produced, CA95 cells showed about twice the activity of the wild-type cells, while Δglo1 and Δglo2 cells had less than 60% of the activity found in wild-type cells (Fig. 4A). Δglo3 cells displayed an intermediate activity.

The kinetics of oxidation of MG showed a lag-phase of about an hour (Fig. 4C), most probably because autocatalytic activation of the enzyme by small amounts of H_2O_2 produced by its basal activity is required for the expression of full activity. An apparent K_m-value for MG of 7 mM was determined using the coupled Amplex Red-peroxidase reaction. The pH-optimum of the reaction was between pH 5 and 6.5. At pH values higher than 7.2 no activity could be observed.

To verify the membrane localization of Glo1 activity, cell fractions were prepared from wild type, Δglo1 and CA95 strains, and their glyoxal oxidase activities were determined. Despite partial loss of activity during preparation of the membrane fractions, membranes of the Glo1-overproducing strain showed a significantly higher activity than membranes from Δglo1 cells (Fig. 4B). Some 80% of this enzymatic activity can be attributed to the membrane fraction of CA95 cells (Fig. 4B). For the other strains, enrichment was observed but was less pronounced. Thus the membrane association could be confirmed by an enrichment of enzymatic activity upon cell fractionation.

The substrate specificity of Glo1

To investigate the substrate specificity of Glo1, a series of carbonyls, sugars and alcohol derivatives were incubated with Um518 and CA95 cells, and the supernatants were assayed for the production of H_2O_2. Comparison of the results for CA95 cells and wild-type cells indicated that MG was the preferred substrate, while glycolaldehyde, formaldehyde, dihydroxyacetone and hydroxyacetone were converted at lower rates (Table 3). No activity was observed when sugars were supplied as substrates. The substrate specificity of the membrane fraction was similar, but, in addition, a weak conversion activity was observed for acetaldehyde, glyoxalate, glyceraldehyde and glyoxal (not shown).

The effect of MG, H_2O_2 and detergent on the growth of Um518 Δglo1 mutants and wild-type (Um518) strains

To obtain insights into the biological function of Glo1 in *U. maydis*, the tolerance of wild-type, CA95 and Um518 Δglo1 strains towards MG, H_2O_2 and detergent was investigated. Strains were tested in an agar diffusion assay with filter disks soaked with H_2O_2, MG and SDS, respectively. Wild-type cells showed the highest tolerance to H_2O_2 and MG; the Δglo1 strain was more sensitive to MG. Unexpectedly, CA95 showed the highest sensitivity to both substrates (Fig. 5). The reason for this phenotype remains unclear, but it may be that stringent regulation of the enzymatic activity is required in order to detoxify MG and, at the same time, prevent the production of toxic amounts of H_2O_2. With respect to detergent sensitivity, wild-type cells, Δglo2, Δglo3 and CA 95 cells showed less sensitivity to SDS, while the growth of Δglo1 cells was inhibited by 2.5% SDS, probably due to their cell wall defect.

Furthermore, we stained wild-type and Um521Δ *glo1* cells with Calcofluor, which labels β-1,3-glucans. In

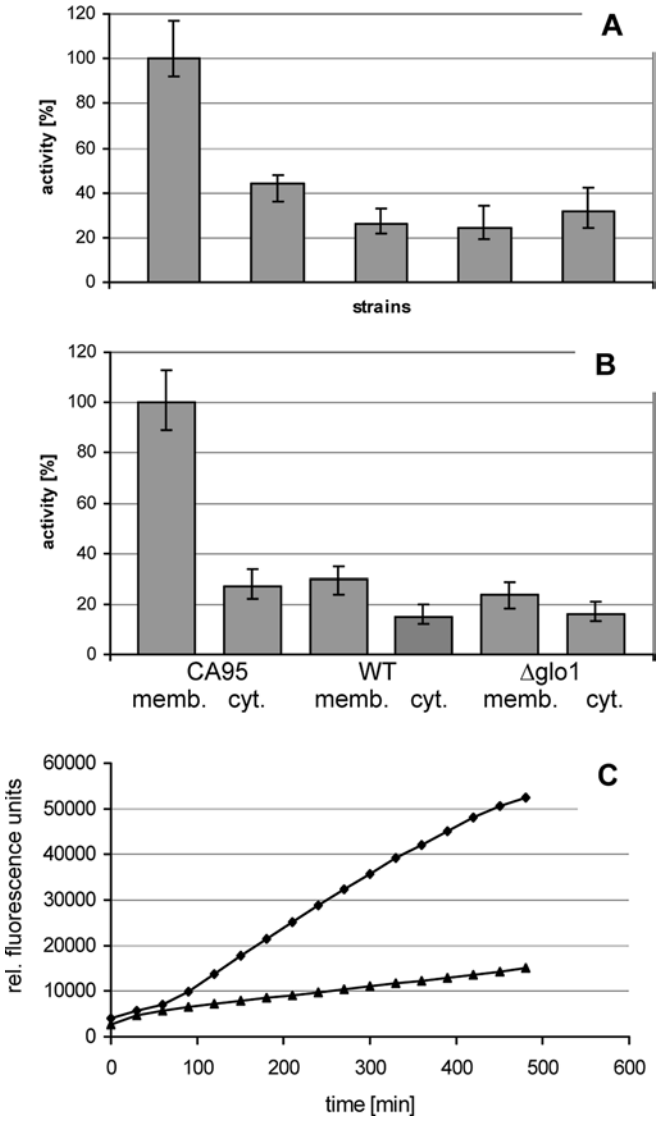

Fig. 4A–C Glo1 produces H_2O_2 with MG as substrate. Production of H_2O_2 was determined fluorimetrically, using the Amplex red-peroxidase-system, as an increase in fluorescence at 595 nm (excitation at 550 nm). Reactions were started by the addition of MG. The activity of CA95 was set to 100%. The mean values of eight independent experiments are shown, and each experiment was performed twice. **A** Relative activity of Glo1 in (from left to right) CA95, Δ *glo1*, Δ *glo2*, Δ *glo3* and Um518 cells was determined after 9 h of incubation. **B** Membrane fractions and cytosol preparations were assayed for H_2O_2 production in the presence of MG. Strains are indicated *below* the histogram. The efficiency of fractionation was checked by assaying for GAPDH (activity was detected only in the cytosol (not shown). **C** Kinetics of the appearance of Glo1 activity in CA95 cells (*diamonds*) and Um518 cells (*triangles*) as a control. The time course of the relative fluorescence of the derived resorufin derivative is shown

wild-type cells Calcofluor staining was seen in regions where cells divide (bud necks) or where cells are elongating (bud tips). Dividing cells showed two regions of staining close to each other, one in the mother and one in the daughter cell. In Δ *glo1* mutant cells the *β*-1,3-glucan staining is somewhat different. Single cells were often stained at both ends. In cell clusters sometimes all

Table 3 Glo1 activity with different substrates

Substrate	Strain	
	CA95	Wild type
Methylglyoxal (MG)	100	30
Short chain alcohols, glycerol	-	-
Formaldehyde	96	-
Acetaldehyde	-	-
Sugars	-	-
Glycolaldehyde	54	-
Glyoxal	-	-
Glyoxalate	-	-
Glycerolaldehyde	-	-
Di-, Hydroxyacetone	77	20
Malonaldehyde	-	-
Glutaraldehyde	30	-
Pyruvate	-	-

Rates of conversion of different substrates (final conc. 2 mM/10 mM) were measured in the presence of whole CA95 or wild-type cells. H_2O_2-production was determined in phenol red tests (see Materials and methods). MG activity of CA95 was set to 100% for both experiments. Experiments were done in triplicate; values are mean values of two independent measurements.

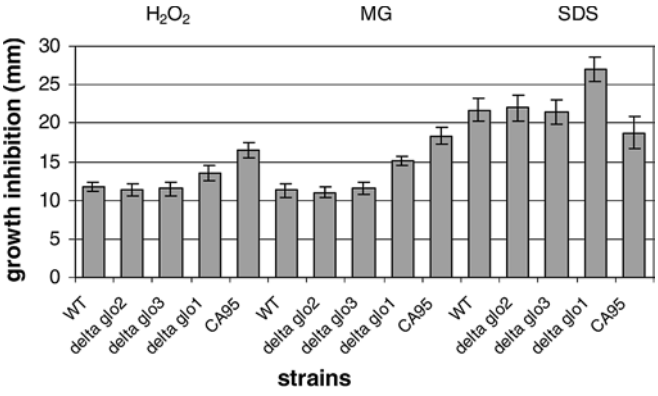

Fig. 5 Agar diffusion test with the strains CA95, Um518, Δ *glo1*, Δ *glo2* and Δ *glo3*. Strains were plated on PD medium, and Whatman filter disks (5 mm) spotted with 1 µl of H_2O_2 (10%-solution) (columns 1–5), 1 µl of MG (40%-solution) (columns 6–10) or 25 µl of SDS (2.5%-solution) (columns 11–15) were placed on the membranes (13 mm). The size of halos of non-growing cells were measured in eight duplicates for each concentration

cell tips displayed staining. Septa, and buds emerging from septa, were intensely stained. This is compatible with the idea that deletion of *glo1* might cause defects during cell wall assembly which enhance the cell's ability to take up Calcofluor (Fig. 2C).

Discussion

Molecular analysis of an insertional mutant of the corn smut pathogen *U. maydis* has identified a glyoxal oxidase-encoding gene, *glo1* , as an important determinant of cell morphology and virulence. Haploid *glo1* deletion mutants proliferate at normal rates, but display a particular morphology: cells appear crumpled, or elongated

with bubbles and with strong vacuolization, form extra septa and exhibit a cytokinesis defect. *glo1* mutant strains fail to form dikaryotic filaments, but they are not sterile. Furthermore, *glo1* mutants are completely non-pathogenic.

Interestingly a targeted mutant of *Botrytis cinerea* with a deletion in a glyoxal oxidase gene also shows severe defects in conidial germination and hyphal growth, specifically on minimal medium. In a test of phytopathogenicity this mutant is completely non-pathogenic on some fruits and ornamentals (J. van Kan, personal communication).

Fungal glyoxal oxidases have so far been described only in the white rot fungus *P. chrysosporium* (Kersten and Kirk 1987; Kersten et al. 1995). There, Glx is an essential component of the lignin degradation pathway, and provides extracellular hydrogen peroxide as a co-substrate for lignin peroxidase and Mn-dependent peroxidase (Janse et al. 1998). Glyoxal oxidases catalyse the enzymatic oxidation of a variety of simple dicarbonyl and β-hydroxycarbonyls, especially glyoxal and methylglyoxal (MG), to carboxylic acids (Kersten and Cullen 1993). This class of enzymes contains an unusual free radical-coupled copper active site (Whittaker et al. 1996, 1999). Its members share a characteristic catalytic motif of four amino acid ligands coordinating to the copper ion: two histidine and two tyrosine residues (Fig. 1A). One of the tyrosines is cross-linked to a cysteinyl residue, forming a thioether dimer that has been shown to be the radical redox site of the enzyme. The best studied member of this enzyme family is the fungal galactose oxidase Galox1 from *Dactylium dendroides*, whose three-dimensional structure has been solved (Ito et al. 1991). Bioinformatic analysis (see Supplementary Material) demonstrates that all fungal proteins, and eight deduced proteins from *A. thaliana*, share the above-mentioned catalytic motif with the conserved histidine and tyrosine residues. The galactose oxidase from *Aspergillus fumigatus* (aspfu_gao1) appears to be an exception, as deduced by automated protein prediction by the Sanger Centre. Our own more detailed analysis (which will be published elsewhere), however, suggests that the first conserved tyrosine is also present.

Glo1 shows significant similarity to the *P. chrysosporium* enzymes Glx1 and Glx2. The *U. maydis* genome contains two additional ORFs that share a high degree of similarity to glyoxal oxidases. These genes, *glo2* and *glo3*, are not involved in pathogenic development, since null mutants cause no change in symptoms after infection of corn seedlings (Table 2). Comparison of Glo1, Glo2 and Glo3 sequences suggest different cellular distributions for these enzymes, which may be decisive for their functions. A fourth ORF (UM02809.1) with less pronounced similarity is also present in the *U. maydis* genome. This ORF encodes a protein which is predicted to be a galactose oxidase (Gao1).

When tested for its substrate spectrum, Glo1 showed the highest activities on MG and glycolaldehyde, whereas other small carbonyls are only poorly utilized. The glyoxal oxidases of *P. chrysosporium*, Glx, show a similar substrate spectrum but less specificity (Kersten and Kirk 1987). Interestingly, the enzymes from both organisms do not use substrates with more than four C atoms, including most abundant sugars. The similarity in the substrate spectrum, and the conservation of catalytic residues, may support a similar reaction mechanism for both enzymes. Heterologously expressed glyoxal oxidase from *P. chrysosporium* needs to be oxidized in order to show full activity (Kersten and Cullen 1993). *U. maydis* Glo1 activity also shows a lag-phase that is probably due to a comparable requirement for autocatalytic activation by small amounts of H_2O_2. The glyoxal oxidase background activity in Δglo1 strains might result from an overlapping activity of other aldehyde-oxidizing enzymes in *U. maydis*.

One possible role for Glo1 that can be derived from the known function of Glx in *P. chrysosporium* is the production of H_2O_2 as a driving force for a second enzymatic reaction. The morphological phenotype of *glo1* mutants suggests that cell wall-modifying activities might require H_2O_2 production by Glo1. It is tempting to speculate that Glo1 might function in the maturation of cell walls, e.g. in the introduction of cross-links. In agreement with this idea, *glo1* mutants are more sensitive to protoplasting enzymes and detergents than are wild-type cells (Fig. 5). In addition, the activity of Glo1 is predominantly membrane associated, and studies of a GFP fusion with Glo1 show that the enzyme is localized especially at the tips of young buds (Figs. 2B and 4B).

An additional function of glyoxal oxidase or its isoenzymes may be the detoxification of MG. Accumulation of methyl glyoxal leads to severe cell damage (Kalapos 1999), although MG is generated in low concentrations during normal metabolism as a by-product of amino acid catabolism and glycolysis, and can account for 0.3% of the total glycolytic flux in *Saccharomyces cerevisiae* (Martins et al. 2001). To prevent cell damage, several detoxification systems for MG exist in nature. In many organisms, from yeast to mammals, this function is provided by the glyoxalase system. The *U. maydis* genome contains a glyoxalase homologue that could potentially detoxify intracellularly produced MG. However, organisms like *P. chrysosporium* are additionally exposed to extracellular sources of MG. Detoxification of extracellular MG is therefore a possible function of glyoxal oxidases. However, cells harboring a glyoxal oxidase detoxification system produce cytotoxic H_2O_2. In *U. maydis,* wild type cells are less sensitive to MG and H_2O_2 than the Glo1 overproducer and the null mutant. This may be because stringent regulation of the enzymatic activity is required in order to detoxify MG and, at the same time, prevent the production of toxic amounts of H_2O_2.

Glo1 might also function in signaling pathways that regulate filamentous growth. Initial experiments presented in this communication do not indicate any influence of Glo1 on the filamentous growth of protein kinase A-deficient strains. However, Glo1 might be

involved in the regulation of filamentous growth and pathogenicity by generating hydrogen peroxide as a messenger or as a source of more active superoxide radicals. One general theory postulates a requirement for an unstable hyperoxidant state to trigger differentiation in many microorganisms. In *Neurospora crassa* and *A. nidulans*, Toledo et al. (1995) and Navarro et al. (1996) showed that a hyperoxidative state occurs at the onset of all morphogenetic processes during conidiation. For plants it has been shown that NADPH oxidases control cell expansion and polarized growth of root hair cells by generating ROS (reactive oxygen species), thereby regulating the activity of calcium channels (Foreman et al. 2003). Recently, Lara-Ortiz et al. (2003) were able to demonstrate the same function of NADPH oxidases in the filamentous fungus *A. nidulans*. Here the production of ROS in the external walls was found to be essential for the differentiation of sexual fruiting bodies. Thus evidence for the importance of ROS as signals in the regulation of diverse cellular processes in fungal physiology and differentiation is accumulating.

To explain the pathogenicity defect of *glo1* mutants, one could also envision a scenario in which H_2O_2 production by Glo1 activity might be essential for successful infection. For the necrotrophic plant pathogenic fungus *B. cinerea,* it has been previously shown that hydrogen peroxide stimulates lesion formation and lesion expansion (Govrin and Levine 2000). Furthermore, a deletion mutant of *B. cinerea* that is defective in superoxide dismutase, another enzyme that produces H_2O_2, shows a strong reduction in pathogenicity (P. Tudzynski, personal communication).

Further investigations into the biological role of glyoxal oxidase should enable us to gain new insights into the processes of filamentous growth and pathogenicity in fungi.

References

Banuett F, Herskowitz I (1989) Different a alleles of *Ustilago maydis* are necessary for maintenance of filamentous growth but not for meiosis. Proc Natl Acad Sci USA 86:5878–5882

Bölker M, Urban M, Kahmann R (1992) The a mating type locus of *U. maydis* specifies cell signalling components. Cell 68:441–450

Bölker M, Böhnert HU, Braun K-H, Görl J, Kahmann R (1995a) Tagging pathogenicity genes in *Ustilago maydis* by restriction enzyme-mediated integration (REMI). Mol Gen Genet 248:547–552

Bölker M, Genin S, Lehmler C, Kahmann R (1995b) Genetic regulation of mating and dimorphism in *Ustilago maydis*. Can J Bot 73:S320–S325

Brachmann A, Weinzierl G, Kämper J, Kahmann R (2001) Identification of genes in the bW/bE regulatory cascade in *Ustilago maydis*. Mol Microbiol 42:1047–1063

Brachmann A, Koenig J, Julius C, Feldbruegge M (2004) A reverse genetic approach for generating gene replacement mutants in *Ustilago maydis*. Mol Gen Genomics 272:216–226

Dürrenberger F, Wong K, Kronstad JW (1998) Identification of a cAMP-dependent protein kinase catalytic subunit required for virulence and morphogenesis in *Ustilago maydis*. Proc Natl Acad Sci USA 95:5684–5689

Foreman J, Demidchik V, Bothwell JHF, Mylona P, Miedema H, Torres MA, Linstaed P, Costa S, Brownlee C, Jones JDG, Davies JM, Dolan L (2003) Reactive oxygen species produced by NADPH oxidase regulate plant cell growth. Nature 422:442–446

Giasson L, Kronstad JW (1995) Mutations in the *myp1* gene of *Ustilago maydis* attenuate mycelial growth and virulence. Genetics 141:491–501

Gillissen B, Bergemann J, Sandmann C, Schroeer M, Bölker M, Kahmann R (1992) A two-component regulatory system for self/non-self recognition in *Ustilago maydis*. Cell 68:647–657

Gold S, Duncan G, Barrett K, Kronstad J (1994) cAMP regulates morphogenesis in the fungal pathogen *Ustilago maydis*. Genes Dev 8:2805–2816

Govrin EM, Levine A (2000) The hypersensitive response facilitates plant infection by the necrotrophic pathogen Botrytis cinerea. Curr Biol 10:751–757

Hoffman CS, Winston F (1987) A ten-minute DNA preparation from yeast efficiently releases autonomous plasmids for transformation of *Escherichia coli*. Gene 57:267–272

Holliday R (1974) Molecular aspects of genetic exchange and gene conversion. Genetics 78:273–287

Ito N, Phillips SE, Stevens C, Ogel ZB, McPherson MJ, Keen JN, Yadav KD, Knowles PF (1991) Novel thioether bond revealed by a 1.7 Å crystal structure of galactose oxidase. Nature 350:87–90

Janse JHB, Gaskell J, Akhtar M, Cullen D (1998) Expression of *Phanerochaete chrysosporium* genes encoding lignin peroxidases, manganese peroxidases, and glyoxal oxidase in wood. Appl Environ Microbiol 64:3536–3538

Kahmann R, Steinberg G, Basse C, Feldbrügge, M, Kämper J (2000) *Ustilago maydis*, the causative agent of corn smut disease. In: Kronstad JW (ed) Fungal pathology. Kluwer Academic Publishers, Dordrecht, pp. 347–371

Kalapos MP (1999) Methylglyoxal in living organisms. Chemistry, biochemistry, toxicology and biological implications. Toxicol Lett 110:145–75

Kämper J (2003, 2004) A PCR-based system for highly efficient generation of gene replacement mutants in *Ustilago maydis*. DOI 10.1007/s00438-003-0962-8 Mol Gen Genomics 271:103–110

Keon JP, White GA, Hargraves JA (1991) Isolation, characterization and sequence of a gene conferring resistance to the systemic fungicide carboxin from the maize smut pathogen Ustilago maydis. Curr Genet 19:475–481

Kersten JP, Cullen D (1993) Cloning and characterization of a cDNA encoding glyoxal oxidase, a hydrogen peroxide-producing enzyme from the lignin-degrading basidiomycete *Phanerochaete chrysosporium*. Proc Natl Acad Sci USA 90:7411–7413

Kersten PJ, Kirk TK (1987) Involvement of a new enzyme, glyoxal oxidase, in extracellular hydrogen peroxide production by *Phanerochaete chrysosporium*. J Bac 169:2195–2201

Kersten JP, Witek C, Van den Wymelenberg A, Cullen D (1995) *Phanerochaete chrysosporium* glyoxal oxidase is encoded by two allelic variants: structure, genomic organization, and heterologous expression of *glx1* and *glx2*. J Bacteriol 177:6106–6110

Klein RD, Gu Q, Goddard A, Rosenthal A (1996) Selection for genes encoding secreted proteins and receptors. Proc Natl Acad Sci USA 93:7108–7113

Krüger J, Loubradou G, Regenfelder E, Hartmann A, Kahmann R (1998) Crosstalk between cAMP and pheromone signalling pathways in *Ustilago maydis*. Mol Gen Genet 260:193–198

Lara-Ortiz T, Riveros-Rosas H, Aguirre J (2003) Reactive oxygen species generated by microbial NADPH oxidase NoxA regulate sexual development in *Aspergillus nidulans*. Mol Microbiol 50:1241–1255

Lau GW, Hamer JE (1998) *Acropetal*: a genetic locus required for conidiophore architecture and pathogenicity in the rice blast fungus. Fungal Genet Biol 24:228–239

Lehmler C, Steinberg G, Snetselaar KM, Schliwa M, Kahmann R, Bölker M (1997) Identification of a motor protein required for filamentous growth in *Ustilago maydis*. EMBO J 16:3464–3473

Martinez D, Larrondo LF, Putnam N, Gelpke MDS, Huang K, Chapman J, Helfenbein KG, Ramaiya P, Detter JC, Larimer F, Coutinho PM, Henrissat B, Berka R, Cullen D, Rokhsar D (2004) Genome sequence of the lignocellulose degrading fungus *Phanerochaete chrysosporium strain* RP78. Nat Biotechnol 22:695–700

Martins AM, Cordeiro CA, Ponces Freire AM (2001) In situ analysis of glyoxalase I and glyoxalase II in *Saccharomyces cerevisiae*. FEBS Lett 499:41–44

Müller P, Aichinger C, Feldbrügge M, Kahmann R (1999) The MAP kinase Kpp2 regulates mating and pathogenic development in *Ustilago maydis*. Mol Microbiol 34:1007–1017

Nakai K, Horton P (1999) PSORT: a program for detecting sorting signals in proteins and predicting their subcellular localization. Trends Biochem Sci 24:34–36

Navarro RE, Stringer MA, Hansberg W, Timberlake WE, Aguirre J (1996) *catA*, a new *Aspergillus nidulans* gene encoding a developmentally regulated catalase. Curr Genet 29:352–359

Paiva S, Kruckeberg AL, Casal M (2002) Utilization of green fluorescent protein as a marker for studying the expression and turnover of the monocarboxylate permease Jen1p of *Saccharomyces cerevisiae*. Biochem J 363:737–744

Petersson J, Pattison J, Kruckeberg AL, Berden JA, Persson BL (1999) Intracellular localization of an active green fluorescent protein-tagged Pho84 phosphate permease in *Saccharomyces cerevisiae*. FEBS Lett 462:37–42

Pick E, Mizel D (1981) Rapid microassays for the measurement of superoxide and hydrogen peroxide production by macrophages in culture using an automatic enzyme immunoassay reader. J Immunol Methods 46:211–226

Romeis T, Brachmann A, Kahmann R, Kämper J (2000) Identification of a target gene for the bE-bW homeodomain protein complex in *Ustilago maydis*. Mol Microbiol 37:54–66

Sambrook J, Fritsch EF, Maniatis T (1989) Molecular cloning: a laboratory manual. Cold Spring Harbor Laboratory Press, Cold Spring Harbor, N.Y.

Schiestl RH, Petes TD (1991) Integration of DNA fragments by illegitimate recombination in Saccharomyces cerevisiae. Proc Natl Acad Sci USA 88:7585–7589

Schulz B, Banuett F, Dahl M, Schlesinger R, Schäfer W, Martin T, Herskowitz I, Kahmann R (1990) The *b* alleles of *Ustilago maydis*, whose combinations program pathogenic development, code for polypeptides containing a homeodomain-related motif. Cell 60:295–306

Spellig T, Bölker M, Lottspeich F, Frank RW, Kahmann R (1994) Pheromones trigger filamentous growth in *Ustilago maydis*. EMBO J 13:1620–1627

Spellig T, Bottin A, Kahmann R (1996) Green fluorescent protein (GFP) as a new vital marker in the phytopathogenic fungus *Ustilago maydis* . Mol Gen Genet 252:503–509

Toledo I, Rangel P, Hansberg W (1995) Redox imbalance at the start of each morphogenetic step of *Neurospora crassa* conidiation. Arch Biochem Biophys 319:519–524

Tsukada T, Carleton S, Fotherinham S, Holloman WK (1988) Isolation and characterization of an autonomously replicating sequence from *Ustilago maydis*. Mol Cell Biol 8:3703–3709

Wedlich-Soldner R, Schulz I, Straube A, Steinberg G (2002) Dynein supports motility of endoplasmic reticulum in the fungus *Ustilago maydis*. Mol Biol Cell 13:965–977

Whittaker MM, Kersten JP, Nakamura N, Sanders-Loehr J (1996) Glyoxal oxidase from *Phanerochaete chrysosporium* is a new radical-copper oxidase. J Biol Chem 271:681–687

Whittaker MM, Kersten PJ, Cullen D, Whittaker JW (1999) Identification of catalytic residues in glyoxal oxidase by targeted mutagenesis. J Biol Chem 274:36226–36232